J Appl Phycol (2016) 28:1085–1095
DOI 10.1007/s10811-015-0642-1

Standard flow cytometry as a rapid and non-destructive proxy for cell nitrogen quota

Martino E. Malerba[1,2,3,4] · **Sean R. Connolly**[3,5] · **Kirsten Heimann**[3,4]

Received: 3 May 2015 / Revised and accepted: 3 June 2015 / Published online: 13 June 2015

Abstract The intracellular concentration of internal nitrogen (the "cell nitrogen quota") is crucial to explain the rate at which phytoplankton populations grow. Hence, understanding changes in cell nitrogen quota is informative on aquatic primary productivity, phytoplankton ecology, eutrophication, and algal blooms. However, current methods to directly monitor per-cell nitrogen quota remain inaccurate, expensive, and time consuming. This study tested the hypothesis that nitrogen limitation triggers systematic optical changes in single cells, which can be rapidly and accurately monitored with a standard flow cytometer. The freshwater microalgae *Desmodesmus armatus*, *Mesotaenium* sp., *Scenedesmus obliquus*, and *Tetraëdron* sp. were reared in nitrogen-limited batch culture conditions across two treatments of initial population densities and monitored for cell nitrogen quota, medium nitrogen, and optical flow cytometric properties of red fluorescence and forward and side light scatters. Changes in nitrogen quota could be described with high accuracy (R^2=0.9) from observations of flow cytometric variables and medium nitrogen, and the relationship did not change across different species or initial population sizes. Red fluorescence was the most important variable explaining 77 % of the total variability in total cell nitrogen and up to 87 % when combined with side light scatter, the second most important variable. Our results indicate that optical flow cytometric variables are a convenient and reliable method to estimate nitrogen quota in microalgal cells.

Keywords Nitrogen status · Optical properties · Chlorophyta · Fluorescence · Nitrogen limitation · Flow cytometry

✉ Martino E. Malerba
martino.malerba@gmail.com

[1] AIMS@JCU, James Cook University, Townsville, Queensland, Australia

[2] Australian Institute of Marine Science (AIMS), Townsville, QLD, Australia

[3] College of Marine and Environmental Sciences, James Cook University, Townsville 4810, QLD, Australia

[4] Centre for Sustainable Tropical Fisheries and Aquaculture, James Cook University, Townsville, QLD 4810, Australia

[5] Australian Research Council Centre of Excellence for Coral Reef Studies, James Cook University, Townsville, QLD, Australia

Introduction

Identifying nitrogen limitation and quantifying the degree of nitrogen stress in phytoplankton cells is of primary importance in ecological and applied phytoplankton fields. Nitrogen is the nutrient required in highest amounts for cell division and is often the first to become limiting. A limiting nutrient is defined as the element whose availability inside the cell is the lowest in relation to the cell's requirement (typically nitrogen, phosphorous, or iron; Howarth 1988). The capacity of a species to store internal nitrogen (here referred as "cell nitrogen quota") is a main determinant of primary productivity, nutrient competition outcomes, and a key mechanism for the maintenance of phytoplankton diversity (Grover 1991; Holt 2008). Furthermore, especially in oligotrophic waters, a sudden release of nitrogen can lead to increasing chances of an algal bloom, often with negative ecological and economic consequences (Cloern 2001). Therefore, substantial resources are allocated to monitor changes in phytoplankton nitrogen content, in order to regulate nitrogen loading budgets from anthropogenic activities (Shelly et al. 2010). Changes in phytoplankton nitrogen quotas are also routinely monitored in algal

aquaculture practices: an intermediate degree of nitrogen limitation is needed to balance the quality (i.e., stress-related increase in lipid and carbohydrate contents) and quantity of the final product (Adams et al. 2013).

Current techniques to determine phytoplankton nitrogen status can be divided into direct and indirect methods, both with limited employability (Shelly et al. 2010; Beardall et al. 2001). The two most common direct methods are elemental analysis and digestion protocols. These techniques quantify the absolute and relative concentrations of single elements in biomass samples and infer the nitrogen quota of single cells (e.g., Li et al. 2014; Bertilsson et al. 2003; Raimbault et al. 1999). However, direct techniques tend to be costly, rely on sophisticated instruments, and, most importantly, cannot differentiate between elements derived from live and dead cells or inorganic particles, which can substantially overestimate per-cell nutrient composition (Beardall et al. 2001). Alternatively, indirect methods to quantify nitrogen status consist of "bioassays" or "enrichment experiments," where the degree of nitrogen limitation is determined by comparing the response (usually growth rate, but also changes in protein content or specific enzymatic activities) of an indicator species (or of a community of species) in a sample when re-supplied with nitrogen (e.g., Hecky and Kilham 1988; Hayes et al. 1984; Dodds et al. 1993). Compared to direct methods, indirect techniques generally do not rely on costly equipment and can exclude the contribution from non-autotrophic particles. However, these experiments are more time consuming (lasting up to weeks) and their results are more controversial due to influences associated with extended confinement of natural assemblages in bottles (Beardall et al. 2001; Shelly et al. 2010; Graziano et al. 1996). Collectively, these shortcomings highlight the need for a reliable and more rapid method to quantify nitrogen status in phytoplankton communities.

An alternative way to improve current estimation techniques for phytoplankton nitrogen limitation is through the analysis of single-cell optical properties. Nitrogen limitation influences many physiological and morphological aspects of phytoplankton cells such as cell volume, cell roundness, pigment composition, quantities of internal organelles, and concentrations of storage molecules (e.g., lipids, carbohydrates, proteins; Vanucci et al. 2010; Rodolfi et al. 2009; Adams et al. 2013; Kolber et al. 1988). The conventional way to quantify cell morphological features is with flow cytometers, which measure optical properties such as light refraction and fluorescence signals as a laser beam excites individual cells (Sosik et al. 2010; Veldhuis and Kraay 2000; Collier 2000). In this way, flow cytometric variables only depend on intrinsic properties of a cell without being influenced by total population size. Three types of flow cytometric optical signals directly relate to the anatomy and physiology of phytoplankton cells. The red fluorescence signal is proportional to the internal concentration of chlorophyll *a* inside the cell and can be used to differentiate phytoplankton cells from chlorophyll-free particulate matter (Sosik et al. 1989; Dubelaar and Jonker 2000). The forward light scatter represents the light travelling along the same axis of the laser beam, and its intensity is proportional to the cell cross section (Dubelaar and Jonker 2000). Finally, the side light scatter represents the light travelling orthogonally to the incident laser beam and its intensity relates to the internal and external structures and granularity of the cell (Dubelaar and Jonker 2000). If the oncoming of nitrogen limitation leads to systematic anatomical and physiological changes within a cell, then, a flow cytometric optical analysis should provide a quantifiable signal for evaluating cell nitrogen quota in ways that are instantaneous, non-destructive, precise, and practical to monitor with automatic programmable instruments.

Optical properties detected with flow cytometers have already been successfully used to infer specific features in phytoplankton cells (Balfoort et al. 1992). The red fluorescence signal accurately ($R^2>0.8$) predicted per-cell concentration of various pigments across different marine phytoplankton species (Cavender-Bares et al. 1999). Furthermore, analysis of forward light scatter signals provided information about the calcification level in coccolithophore cells (von Dassow et al. 2012). Regarding the relationship between optical proprieties and nitrogen status, flow cytometric red fluorescence of *Prochlorococcus*, *Synechococcus*, and picoeukaryotes showed a significant increase following nitrogen addition, which did not occur when supplied with non-limiting iron and phosphorous (Davey et al. 2008). Also, *Microcystis aeruginosa* showed a positive relationship between flow cytometric red fluorescence and medium nitrogen availability (Brookes et al. 2000). Therefore, flow cytometric variables of red fluorescence and forward and side scatter, all appear to be sensitive to changes in nitrogen status across different phytoplankton species and growth conditions.

It is important to consider and account for the effects of photoperiod when evaluating the use of optical properties as a proxy for nutrient status in phytoplankton cells (DuRand and Olson 1998; Mas *et al*. 2008). Photoperiod regulates the cell cycle: formation of cleavage furrows in the cell wall, organelle replication, increase in photosynthetic performance, and change in cell shape and size (Roenneberg and Mittag 1996; Luning 2005). As a result, optical properties of a cell also change depending on cell cycle relative to photoperiod (DuRand and Olson 1998; DuRand *et al*. 2002). Hence, in order to eliminate diurnal effects, data collection was standardized with respect to sampling time.

The aim of this study was to investigate whether cell optical properties measured daily at 18:00 with a standard flow cytometer can be used as an accurate predictor of nitrogen quota in four nitrogen-limited microalgal species *Desmodesmus armatus*, *Mesotaenium* sp., *Scenedesmus obliquus*, and *Tetraëdron* sp. grown in laboratory batch culture. In the experiment, nitrogen-limited cultures were resupplied with nitrate and monitored daily until stationary phase across two treatments of initial inoculation densities. Our results demonstrate that flow cytometric optical properties can serve as excellent proxies for nitrogen quota in laboratory batch cultures.

Material and methods

Monoclonal 1.2 L batch cultures of three green microalgae, *Desmodesmus armatus* (R. Chodat) E. Hegewald (culture accession: NQAIF301), *Scenedesmus obliquus* (Turpin) Kützing (NQAIF299), and *Tetraëdron* sp. (NQAIF295), and one charophyte, *Mesotaenium* sp. (NQAIF303), were sourced from the North Queensland Algal Culturing and Identification Facility at James Cook University (Townsville, QLD). The four species coexist in nature and are among the most common and resilient species in the area where they were originally isolated, at the Tarong Power Station ash-dam (Tarong, Queensland, Australia). Mother cultures were reared in standard Bold Basal Medium (BBM; Nichols 1973). All chemicals for culturing and nutrient analyses were purchased from Sigma-Aldrich. Nitrogen was set as the limiting factor for growth in all experimental cultures, by acclimatizing in nitrogen-free BBM prior to the beginning of the experiments until population density reached stationary phase and successively supplying 1000 μmol-N L^{-1} of sodium nitrate ($NaNO_3$), which represents a third of the original BBM nitrogen concentration. Potential for carbon limitation was minimized by ensuring pH levels below 7 by buffering the modified nitrate-BBM with 4-(2-hydroxyethyl)-1-piperazineethanesulfonic acid (HEPES) at 8 mmol L^{-1} and by supplying $NaHCO_3$ at 2.38 mmol L^{-1}. Cultures were kept in a temperature-controlled room at 27±3 °C with a 14–10-h day-night cycle at a light intensity of 70 μmol photons m^2 s^{-1}. Cultures were continuously mixed with magnetic stirrers at 300 rpm (IKA RCT Basic, IKA Labortechnik, Germany) and aerated with 0.45 μm filtered air (Durapore, Millipore). Glassware was acid-washed (10 % HCl), and all culturing materials were autoclaved and handled aseptically in a laminar flow cabinet.

Experimental design To test for the influence of light penetration and per-cell medium nitrogen availability, two independent replicate cultures for each of the four species were grown at two treatments of initial inoculation densities, leading to different per-cell nitrogen availabilities and mean light penetrations. Culture volume was standardized at 1 L. To standardize initial conditions for biomass and light penetration across species with different cell sizes, starting inoculation cell densities were set at optical densities of 0.01 for the low initial inoculation treatment and were increased fivefold to 0.05 for the high initial inoculation treatments. Initial medium nitrogen was kept constant at 1000 μmol-N L^{-1}, which meant an approximate fivefold difference in per-cell medium nitrogen availability between the two treatments. Inoculation densities were based on preliminary analysis of the species to ensure from 3 to 6 days of fast nitrogen-driven population growth. Optical densities were measured at 750 nm on three 250 μL mother culture samples loaded on standard 96-well plates (EnSpire® Multimode Plate Reader; PerkinElmer, USA).

It is important to consider and account for the effects of photoperiod when evaluating the use of optical properties as a proxy for nutrient status in phytoplankton cells (Mas et al. 2008; DuRand and Olson 1998). Photoperiod regulates the cell cycle: formation of cleavage furrows in the cell wall, organelle replication, increase in photosynthetic performance, and change in cell shape and size (Luning 2005; Roenneberg and Mittag 1996). As a result, optical properties of a cell also change depending on cell cycle relative to photoperiod (DuRand et al. 2002; DuRand and Olson 1998). Hence, data collection was conducted every day at 18:00, in order to control for any diurnal fluctuations.

Flow cytometric analysis Three replicate measurements per culture were taken every day at 18:00 loading 250 μL on a 96-well plate and measured with a Guava EasyCyte flow cytometer (Millipore, USA). Before cytometric analysis, each sample was diluted with deionized (DI) water between 25 and 50 times to maintain the optimal precision range of the instrument (50 to 500 cells μL^{-1}). Optical variables are represented by the mean of the cytometric histograms for red fluorescence, forward scatter, and side scatter. The excitation light was a blue laser at 488 nm and 75 MW, and emission was recorded at 488±6 nm for forward and side light scattering and at 690±50 nm for red fluorescence as individual cells pass through a microcapillary flowcell at 0.1 μL sec^{-1}. Population size and optical coefficients were estimated after excluding dead cells and inorganic particles characterized by low red fluorescence signals. Instrument precision was periodically checked with Guava easyCheck beads (Catalog No. 4500-0025, Millipore), ensuring a coefficient of variation (CV) <5 % for all detectors. Flow cytometric optical values are relative to the voltage applied to the photodetector. We controlled for the sensitivity of the photodetector by keeping it constant throughout all experiments and all species. Moreover, we facilitated result reproducibility by normalizing flow cytometric

readings by the optical mean values of the easyCheck beads, a strategy already adopted by DuRand and Olson (1996, 1998) and Mas et al. (2008).

Medium nitrogen analysis Phytoplankton cells can respond with nitrite (NO_2^-) excretion when initially exposed to a surge of ambient nitrate (NO_3^-; Malerba et al. 2012). Hence, we quantified total medium nitrogen as the sum of nitrate and nitrite ambient concentrations with the ultraviolet spectrometric screening method (Lanoul et al. 2002). Three 1.25 mL replicate samples per culture of filtered supernatant were acidified with 25 μL 1 N HCl to prevent interference from hydroxide or carbonate molecules (Clescerl et al. 1999). After vortexing, 250 μL was transferred onto a 96-well plate (Ultraviolet-Star, Greiner Bio-One GmbH) and optical density was measured at 230 nm (OD_{230}; EnSpire). Also, because certain types of dissolved organic matter can also absorb at 230 nm and NO_3^- and NO_2^- do not absorb at 275 nm, a second measurement at 275 nm (OD_{275}) was used to correct each OD_{230} reading (Clescerl et al. 1999). The standard curve for (OD_{230}–OD_{275}) was linear across the range of nitrogen concentrations used in the experiments ($R^2 \geq 0.995$).

Total particulate nitrogen and cell nitrogen quota Estimation of total particulate nitrogen content was performed by digesting biomass samples and oxidizing all nitrogen to nitrate following the persulfate oxidation method (Eaton et al. 2005; Delia et al. 1977; Solorzano and Sharp 1980) and later estimating total nitrate-only concentration with the salicylate method (Cataldo et al. 1975). Cell nitrogen quota was then estimated for each sample by dividing total particulate organic nitrogen by the population size at each day of the experiment. The persulfate digestion required two reagent solutions: (1) 2.01 g of $K_2S_2O_8$ and 1.5 mL of 5 M NaOH in 100 mL DI water (made fresh daily) and (2) 6.18 g H_3BO_3 and 0.8 g NaOH in 100 mL DI water (stable solution). Nitrate determination with the salicylate protocol required two reagent solutions: (3) 0.5 g of $C_7H_6O_3$ in 10 mL of conc. H_2SO_4 (made fresh daily) and (4) 200 g NaOH in 1 L DI water (stable solution). Inorganic and organic standard nitrogen stocks were (1) 1.011 g KNO_3 in 1 L DI water for the inorganic control and (2) 0.75 g of glycine in 1 L DI water for the organic control.

The procedure for determining total particulate nitrogen consisted of three steps. Firstly, cells were separated from the supernatant by centrifuging between 2 to 14 mL of sample (depending on the total nitrogen content in the sample) at 3000×*g* at 5 °C for 10 min, gently removing 12 mL of supernatant, and re-suspending the biomass by diluting with DI water to a total volume of 14 mL. The procedure was repeated four times and, at the end of the fourth cycle, cells were concentrated in 2 mL. Secondly, biomass digestion was carried out by mixing 2 mL of reagent (1) with the concentrated biomass samples, autoclaving the solution for 30 min at 121 °C, and allowing to rest in the autoclave overnight. We checked that increasing autoclaving time to 45 and to 60 min did not change the digestion efficiency. Thirdly, total nitrate was determined by mixing 300 μL of digested sample and 400 μL of reagent (3), vortexing, and incubating at room temperature for 20 min. Then, 5.7 mL of reagent (4) was added to the solution. Optical density was read at 410 nm after loading 350 μL on a 96-well plate (EnSpire). For each sample, total nitrogen concentration was calculated based on a linear regression from a 7-point calibration curve, made daily from potassium nitrate stock ($R^2 > 0.99$). A second 7-point calibration curve made daily from organic glycine and served as positive control for the persulfate oxidation method.

Statistical analysis A multiple linear regression was carried out to examine daily changes in cellular internal nitrogen as a function of five continuous explanatory variables of per-cell red fluorescence, per-cell forward and side light scatters, medium N concentration, population size, and two categorical explanatory variables of the two experimental initial conditions and the four species. To ensure linearity, red fluorescence, forward light scatter, side light scatter, and population size were natural log transformed, while medium N concentration was square root transformed. To satisfy the assumptions of generalized linear models, we avoided biases due to multicollinearity between main effects by setting a cutoff variance inflation factor value of 5 (Zuur et al. 2009). In the data, all dynamics transitioned from states of high nitrogen-low population size to zero nitrogen-high population size; as a result, the variables for medium nitrogen and population size were highly negatively correlated (variance inflation factor of 12) and could not be both included as explanatory variables in the same model. However, availability of medium nitrogen was clearly the underlying driver: a decrease in irradiance from increased population size and increased self-shading is expected to increase per-cell red fluorescence, due to higher pigmentation from photoacclimatization (Sosik et al. 1989). Conversely, a decrease in medium nitrogen availability should coincide with a decline in cell red fluorescence, due to reduced photosynthetic rate from factors such as reduced N-rich pigments, reduced thylakoid efficiency, decline in photosystem II density, reduction in light-harvesting complex, and a decline in enzymatic activities (Turpin 1991). Because we observed decreasing red fluorescence during the experiments, medium nitrogen is implicated as the driver. Hence, population size was removed from the initial full model and this reduced the maximum variance inflation factor score to 2.7, which was below the assumed cutoff value of 5.

Combinations between the four species and two initial inoculation densities could produce different interactive effects on optical properties, medium nitrogen, or total cell nitrogen. To

account for this, nine two-way interaction terms were included for all combinations between all continuous variables and the categorical explanatory variables of species and initial population size (also including an interaction term between the two categorical variables). Furthermore, three additional interaction terms were included between all combinations of optical properties with each other, to account for likely interactions between physical properties of a cell (e.g., fluctuations in red fluorescence can depend on changes in forward or side light scatters). Overall, 31 estimated parameters were included in the initial full model, with a total of 89 residual degrees of freedom. Standard diagnostic plots on model residuals were examined to ensure normality (QQ plot), homoscedasticity (standardized residuals vs. fitted values) and absence of influential observations or outliers (Cook's distance <0.5). Bayesian information criterion (BIC; Schwarz 1978) was adopted to determine the best-fitting model from all possible candidates, obtained by removing single or combination of parameters from the initial fully parameterized model. The best-fitting model following BIC model selection is the one that minimizes the formula: $-2 \times L + 2 \times k \times (ln(n) - ln(2\pi))$, where L is the maximum likelihood score, k is the total number of calibrated parameters, and n is the sample size. ΔBIC was then calculated by subtracting the BIC score of the best model from all other scores (i.e., the ΔBIC for the best model is 0). In general, models with ΔBIC between 0 and 2 should be considered as having substantial empirical support (Kass and Raftery 1995; Strong et al. 1999). Model selection was carried out with the R package MuMIn (Barton 2014).

For the best-fitting model selected by BIC, the independent contribution of each explanatory term to the total explained variability was calculated with the hierarchical partitioning method (HPM) by Chevan and Sutherland (1991). The HPM method isolates the unique contribution of each single variable in a multiple regression analysis. For example, the contribution of variable U to the total R^2 of a multiple regression including U, V, Y, and Z is calculated by evaluating the incremental improvement in total explained variance $\left(R_U^2\right)$ when introducing U to all possible model configurations, averaged within a certain model size (i.e., first order: V, Y, Z; second order: VZ, YZ, VY; third order: VYZ). Finally, the unique contribution of U to the total R^2 in the multiple regression is calculated by taking the average of the three R_U^2 scores across the first, second, and third orders of model sizes (Gromping 2006). The 95 % confidence intervals (CI) for the relative contributions are calculated by ordinary non-parametric bootstrapping of all observations in the dataset (with replacement) 10^4 times and repeating the HPM method for each bootstrapped dataset (Gromping 2006). HPM and bootstrapped CI were calculated with R package relaimpo (Gromping 2006, 2007). Statistical computer software R and RStudio were used for all analyses and graphs (R Core Team 2014; RStudio 2013).

Results and discussion

This study confirmed the hypothesis that flow cytometric optical properties could reveal information about nitrogen quota in laboratory batch cultures. Of all the competing models derived from removing single or combinations of parameters from the starting full model, only one fell within the threshold level of ΔBIC<2 (Table 1). This best-fitting model explained 90.2 % of the changes in cell nitrogen quota as a function of the main effects for all three optical properties (i.e., red fluorescence and forward and side light scatters) and available medium nitrogen (Tables 1 and 2). Model selection did not detect any important main or interactive effects of species (Table 1), implying that the effects of the main explanatory variables were consistent across all four species. Similarly, initial population size was not included in the best model (Table 1), indicating that any effects of different per-cell medium nitrogen availabilities were implicitly accounted for by optical properties and medium nitrogen. The best-fitting model performed very well across all four species and for both initial nitrogen conditions (r=0.87–0.94), showing no evidence of bias (Fig. 1). Red fluorescence had the highest explanatory power in the analysis. The total explained variability in the best-fitting model was 90 %, but optical parameters of red fluorescence, forward scatter, and side scatter contributed to 88 %, and only the remaining 2 % was explained by medium nitrogen (Fig. 2). Indeed, a linear model including only the two most influential explanatory variables, red fluorescence and side scatter, could explain 87 % of the total variability in total cell nitrogen (Fig. 3), of which the overwhelming majority (77 %) could be explained with a simple linear regression only including red fluorescence (Fig. 4). Overall, these results strongly support the hypothesis that optical variables are a potential proxy for nitrogen quota for all four algal species reared in laboratory nitrogen-limited batch culture conditions.

The existence of a relationship between nitrogen quota and cell optical properties is consistent with our understanding of nutrient-limited growth in autotrophic cells. Together with carbon, nitrogen is the element in the highest demand during cell division, and when nitrogen is in short supply, cells respond by relocating nitrogen from storage molecules to vital metabolic functions (Mulholland and Lomas 2008; Dortch et al. 1984). Hence, low nitrogen status usually coincides with a decline in N-rich pigments, density of internal organelles, and decrease in cell size, which are all related to the optical properties recorded with a flow cytometer: the intensity of the red fluorescence signal is mainly proportional to the total pigment concentration (especially chlorophyll *a*), forward light

Table 1 Summary table for the ten best models following Bayesian information criterion (BIC) model selection

Model #	Model terms									
	Intercept	Exp.	log(Fwd)	log(Red)	log(Side)	Species	sqrt(MdN)	Exp:log(Side)	Exp:sqrt(MdN)	log(Fwd):log(Red)
1	−17.77		0.32	0.90	0.35		0.01			
2	−18.21		−0.57	1.06	0.32		0.01			0.39
3	−17.66	+	0.32	0.86	0.37		0.01			
4	−17.95			0.96	0.41		0.01			
5	−18.00		0.36	0.98	0.15		0.01			
6	−17.64	+	0.30	0.83	0.34		0.01	+		
7	−17.74		0.45	0.90	0.37		0.01			
8	−17.87	+	0.30	0.92	0.34		0.01		+	
9	−19.09	+	0.90	1.23	−0.90	+	0.02		+	
10	−17.87	+	0.28	0.89	0.30		0.01	+	+	

Model #	Model terms								
	log(Fwd):log(Side)	log(Fwd):Species	log(Red):log(Side)	log(Side):Species	R^2	df	LogLik	BIC	ΔBIC	Cum. Weight
1					0.90	6	16.38	−4.03	0.00	0.46
2					0.90	7	17.46	−1.42	2.61	0.12
3					0.90	7	17.15	−0.79	3.23	0.09
4					0.89	5	11.97	0.00	4.02	0.06
5			0.07		0.90	7	16.75	0.01	4.04	0.06
6					0.91	8	18.89	0.52	4.55	0.05
7	0.08				0.90	7	16.42	0.68	4.71	0.04
8					0.91	8	18.80	0.71	4.73	0.04
9		+	0.35	+	0.94	18	42.66	0.85	4.88	0.04
10					0.91	9	20.92	1.26	5.28	0.03

Rows represent individual models ordered from lowest to highest BIC score. Columns indicate each model term (main effects or interactions that were selected at least once in the top ten models), coefficient of determination (R^2), degree of freedom (*df*), maximum log-likelihood score (*LogLik*), BIC score, ΔBIC, and cumulative weight. Presence for model terms is indicated with either its estimated parameter value for continuous variables or with a "+" sign for categorical variables. Models were judged based on ΔBIC, calculated by subtracting the overall best BIC score from the scores of each model (hence, by definition, the ΔBIC of the best model is 0). Interaction terms between two variables are represented with the column sign (":")

Exp. the two initial conditions of starting population densities, *Fwd* forward light scatter, *Red* red fluorescence, *Side* side light scatter, *MdN* the available medium nitrogen

Table 2 ANOVA table for the best-fitting multiple linear regression on total cell nitrogen following BIC model selection (see model #1 in Table 1)

Source (transformation)	Sum of squares	df	Mean square	*F* value	Prob (*F*)
Red fluorescence ($\log_e$)	41.8	1	41.8	899.1	<0.0001
Side scatter ($\log_e$)	5.6	1	5.6	119.6	<0.0001
Forward scatter ($\log_e$)	0.5	1	0.5	11.1	<0.0001
Medium N (sqrt)	1.3	1	1.3	28.9	<0.0001
Residuals	5.3	115	0.05		

$F_{4,115}$=265, Prob (*F*) <0.0001; R^2 =0.902, adj. R^2 =0.899

scatter is a proxy for cell cross section and cell volume, and side light scatter is proportional to the general internal complexity of the cell (or its granularity; Dubelaar and Jonker 2000). In principle, similar mechanisms should also apply for cells limited by different nutrients. For instance, positive trends in flow cytometric optical values have been recorded from nutrient-limited cultures resupplied with iron (Zettler et al. 1996; Timmermans et al. 2001; Liu and Qiu 2012; Davey et al. 2008), phosphorous (Demers et al. 1989; Cleveland and Perry 1987), and silicon (Demers et al. 1989).

This is the first documentation of flow cytometric optical properties as a quantifiable proxy for cell nitrogen quota in phytoplankton cells. These findings have implications for the way we monitor phytoplankton species. Firstly, optical properties are among the few measurements that can be quantified non-destructively from phytoplankton cells. This circumvents having to indirectly calculate per-cell concentrations by dividing two estimates for total elemental concentration and total population size, which inevitably leads to propagation and compounding of the uncertainty around the overall mean. Secondly, measuring optical properties in field or laboratory samples easily allow filtering out the contributions from all non-autotrophic particles through the intensity of the red fluorescence signal, which is mainly proportional to the

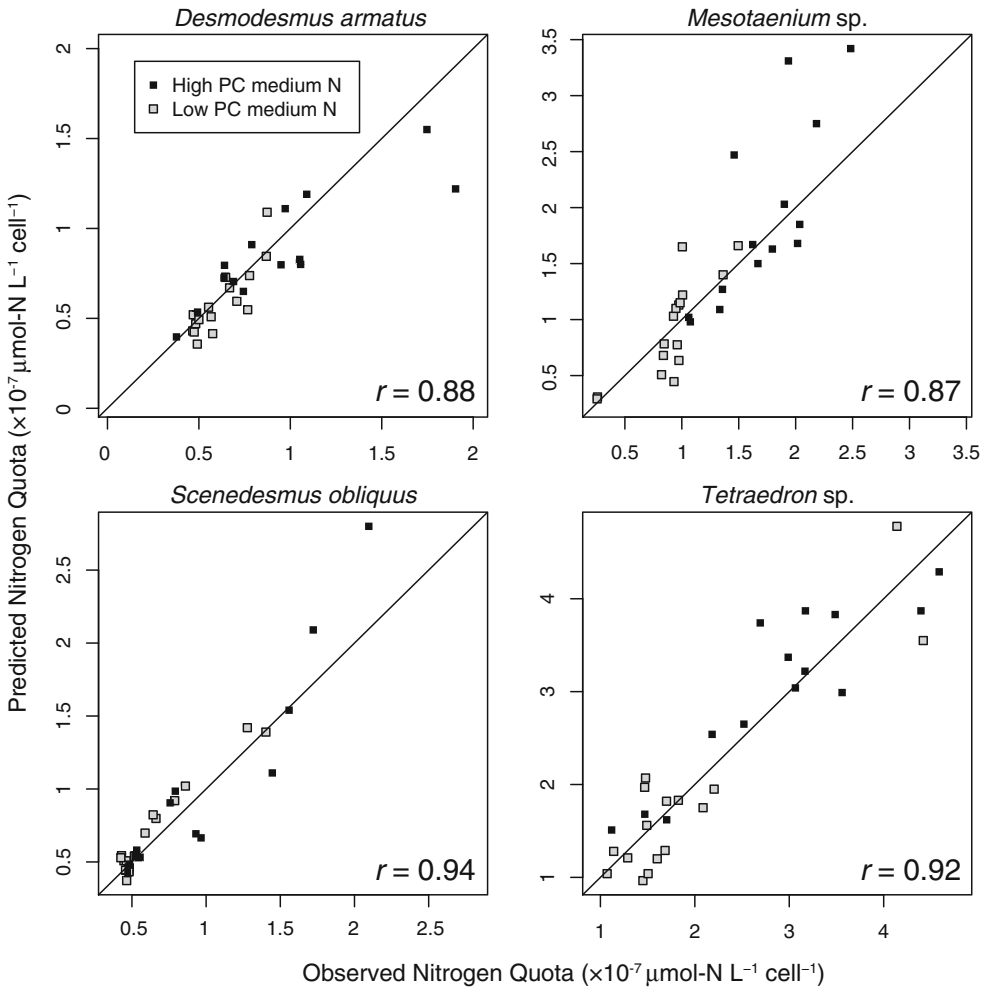

Fig. 1 Observed and predicted nitrogen quota values extracted from the best-fitting model for each species. Each *dot* represents an independent culture for each day of the experiment, with different *symbols* indicating the two different initial per-cell nitrogen availabilities. The correlation coefficient quantifies the goodness of fit for each species pooled across both treatments of initial nitrogen. The *diagonal line* is the unity line, where observed and predicted values are equal

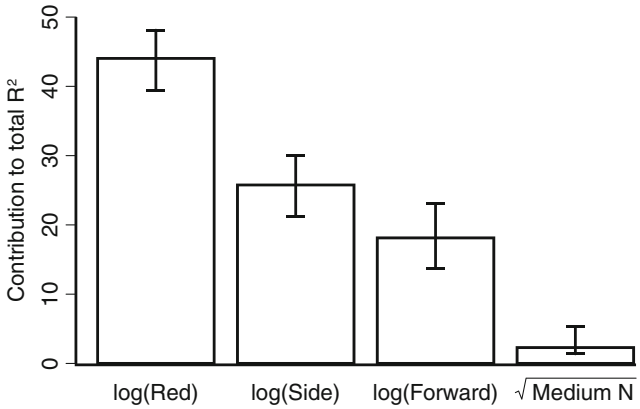

Fig. 2 The unique contribution of explanatory variables for red fluorescence (*Red*), side light scatter (*Side*), forward light scatter (*Forward*), and medium nitrogen (*Medium N*) to the coefficient of determination (R^2±95 % bootstrapped confidence intervals) of the multiple regression model (see Table 1), as calculated by the hierarchical partitioning method (HPM). Total model explained variability (i.e., sum of the four unique contributions) was 90 %

concentration of pigments in photosynthetic tissues (Dubelaar and Jonker 2000). Moreover, it is now technologically feasible to measure phytoplankton optical properties from automated monitoring stations (Thyssen et al. 2014; Zhou et al. 2012). The temporal resolution from such flow cytometric time series can provide important information about the influence of biotic and abiotic factors on nitrogen quota dynamics.

Introducing a protocol for flow cytometric analysis of nitrogen status can also benefit microalgal biotechnological production systems. Imposing a nitrogen-limited regime to a culture can substantially enhance the production of storage lipids (e.g., triacylglycerols) and carbohydrates (mainly starch), leading to a significant increase in the specific value of the microalgal biomass (Ikaran et al. 2015). Today, conventional analytical methods are often implemented for monitoring and optimizing biomass quality, but with results only available considerable time after each sample is taken (da Silva et al. 2012). Only recently, flow cytometric systems for continuous culture monitoring of lipid content, cell size, enzyme activity, and identification of microbial species are starting to emerge (da Silva et al. 2012; Hyka et al. 2013). While not common, such near-instantaneous methods have already produced some improvements in the productivity and the reproducibility of microalgal cultivation processes (de la Jara et al. 2003; Gouveia et al. 2009; Doan and Obbard 2011). Our approach can complement such applications of flow cytometry, by facilitating rapid assessments of culture nitrogen status.

It is important to quantify the variability of the relationship between optical properties and nitrogen quota across different species. Trends in optical properties mainly depend on the relative composition of different types of pigments within a cell (Sosik et al. 1989). Hence, it is likely that taxonomically related species will often show consistent relationships in optical properties. In this study, the calibrated relationship between nitrogen quota and cell optical properties was consistent across three chlorophytes and one charophyte species (BIC selected against species-specific coefficients; see Tables 1 and 2). This means that an increase in internal nitrogen corresponded to the same response in optical properties across all four species. The extent to which this relationship remains consistent across more

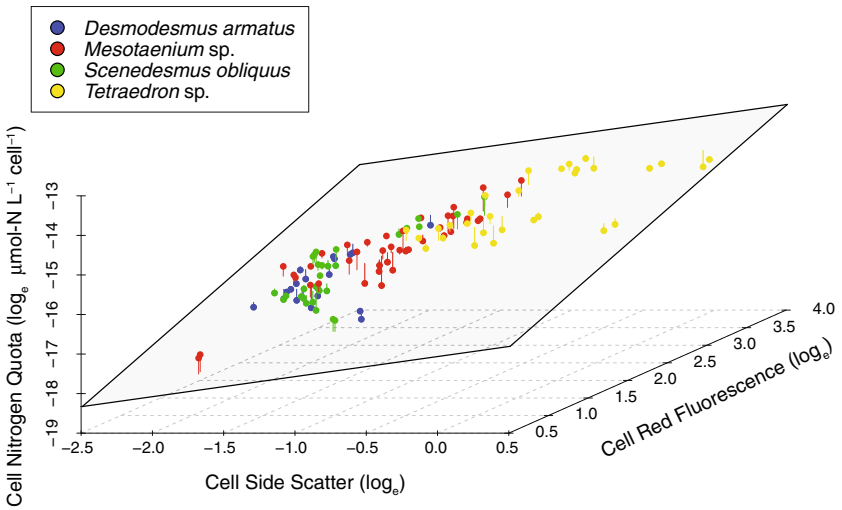

Fig. 3 Multiple linear regression for total cell nitrogen as a function of the two most important model explanatory variables: flow cytometric red fluorescence and side scatter (see Table 1 and Fig. 2). Optical values are in relative units and normalized by mean optical values of the flow cytometric beads. Each *point* is a daily measurement at 18:00 collected from a factorial design of two independent replicate cultures for four species for two initial cell densities (R^2=0.868). *Points* and *perpendicular residuals* to the prediction plane are color-coded for the four different species

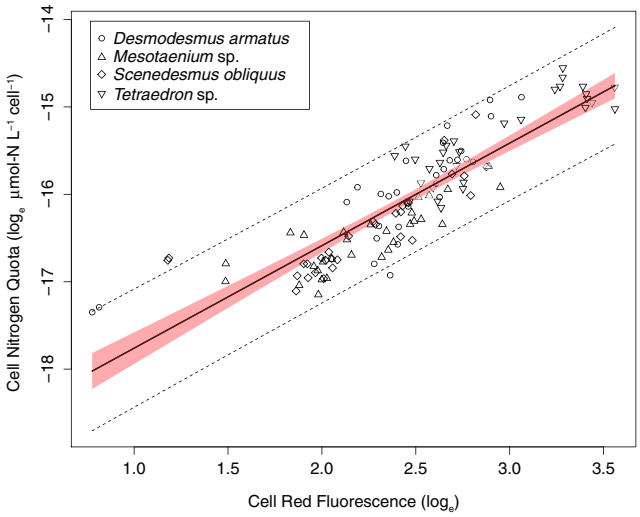

Fig. 4 Linear regression for total cell nitrogen as a function of red fluorescence with 95 % confidence intervals (*red envelop*) and 95 % projection intervals (*dashed lines*). Optical values are in relative units and are normalized by mean optical values of flow cytometric beads. Each *point* is a daily measurement of a species at 18:00 from two independent replicate cultures at two initial cell densities (R^2=0.77)

taxonomically disparate species, however, requires further investigation.

Future research should assess the reliability of optical properties as a proxy for nitrogen quota when extended from laboratory cultures to field samples of mixed assemblages. This requires analyzing the effects of additional covariates, such as the effects of multiple potentially limiting nutrients. Furthermore, cells can photoacclimatize and change their pigment concentrations when exposed to different light intensities (Collier 2000; Dusenberry et al. 1999; Jacquet et al. 1998). Hence, the influence of light irradiance on the relationship between optical properties and nitrogen quota should be calibrated. Finally, optical characteristics also change throughout the diel cycle, usually increasing intensity throughout the light phase (Mas et al. 2008; DuRand and Olson 1998), highlighting the need to standardize for time of sampling. Assessing each individual contribution from these factors can facilitate the comprehensive interpretation of time series of per-cell optical properties with respect to nitrogen quota from field samples.

The capacity of phytoplankton cells to assimilate and store growth-limiting nutrients has important implications in nature and in engineered systems. Presently available techniques for directly measuring nitrogen quota in phytoplankton cells are difficult and not feasible for monitoring frequently or over large areas (Shelly et al. 2010). The use of optical proxies has already revolutionized the scale and frequency of phytoplankton monitoring. For instance, the MODIS spectroradiometer installed on satellites Terra and Aqua documented, for the first time, patterns of global primary production on ocean surfaces by recording total chlorophyll fluorescence as a proxy for phytoplankton biomass (Bordi et al. 1999). Today, flow cytometers are installed in most oceanographic vessels and can even be designed as automated submersible units for continuous monitoring of natural phytoplankton assemblages or microalgal bioreactors (Yentsch et al. 1983; Olson et al. 2003). The results of the present study indicate that flow cytometric data does not just indicate total population size but also has the potential to provide information on nitrogen quota of phytoplankton cells.

Acknowledgments We are grateful to the North Queensland Algal Identification and Culturing Facility (NQAIF), in particular Stan Hudson and Florian Berner. We also thank A/Prof Bruce Bowden and Prof James Burnell for the assistance in laboratory protocols. Finally, we thank Dr Lyndon Llewellyn, Dr Christian Lonborg, Dr Murray Logan, and Dr Catia Carreira for the helpful advice. This research was supported by AIMS@JCU (aims.jcu.edu.au), the Australian Institute of Marine Science (www.aims.gov.au), the Advanced Manufacturing Cooperative Research Centre (Project 2.3.4), and James Cook University (www.jcu.edu.au). We also thank the reviewers, whose comments and suggestions helped improve the manuscript.

References

Adams C, Godfrey V, Wahlen B, Seefeldt L, Bugbee B (2013) Understanding precision nitrogen stress to optimize the growth and lipid content tradeoff in oleaginous green microalgae. Bioresour Technol 131:188–194

Balfoort HW, Berman T, Maestrini SY, Wenzel A, Zohary T (1992) Flow-cytometry—instrumentation and application in phytoplankton research. Hydrobiologia 238:89–97

Barton K (2014) R Package "MuMIn": Model selection and model averaging based on information criteria (AICc and alike)

Beardall J, Young E, Roberts S (2001) Approaches for determining phytoplankton nutrient limitation. Aquat Sci 63:44–69

Bertilsson S, Berglund O, Karl DM, Chisholm SW (2003) Elemental composition of marine *Prochlorococcus* and *Synechococcus*: implications for the ecological stoichiometry of the sea. Limnol Oceanogr 48:1721–1731

Bordi F, Neeck S, Scolese C (1999) Contribution of EOS Terra to Earth science. In: Fujisada H, Lurie JB (eds) Sensors, systems, and next-generation satellites, vol 3870, Proceedings of the Society of Photo-Optical Instrumentation Engineers (Spie). Spie-Int Soc Optical Engineering, Bellingham, pp 260–268

Brookes JD, Geary SM, Ganf GG, Burch MD (2000) Use of FDA and flow cytometry to assess metabolic activity as an indicator of nutrient status in phytoplankton. J Mar Freshw Res 51:817–823

Cataldo DA, Haroon M, Schrader LE, Youngs VL (1975) Rapid colorimetric determination of nitrate in plant-tissue by nitration of salicylic-acid. Commun Soil Sci Plant Anal 6:71–80

Cavender-Bares KK, Mann EL, Chisholm SW, Ondrusek ME, Bidigare RR (1999) Differential response of equatorial Pacific phytoplankton to iron fertilization. Limnol Oceanogr 44:237–246

Chevan A, Sutherland M (1991) Hierarchical partitioning. Am Stat 45: 90–96

Clescerl LS, Greenberg AE, Eaton AD (1999) 4500 NO_3 Nitrogen (Nitrate). In: APHA, AWWA, WPCF (eds) Standard Methods For Examination of Water and Wastewater. 20th edn. Amer Public Health Assn

Cleveland JS, Perry MJ (1987) Quantum yield, relative specific absorption and fluorescence in nitrogen-limited *Chaetoceros gracilis*. Mar Biol 94:489–497

Cloern JE (2001) Our evolving conceptual model of the coastal eutrophication problem. Mar Ecol Prog Ser 210:223–253

Collier JL (2000) Flow cytometry and the single cell in phycology. J Phycol 36:628–644

R Core Team (2014) R: A language and environment for statistical computing. R Foundation for Statistical Computing, Vienna, Austria. URL http://www.R-project.org/

da Silva TL, Roseiro JC, Reis A (2012) Applications and perspectives of multi-parameter flow cytometry to microbial biofuels production processes. Trends Biotechnol 30:225–232

Davey M, Tarran GA, Mills MM, Ridame C, Geider RJ, LaRoche J (2008) Nutrient limitation of picophytoplankton photosynthesis and growth in the tropical North Atlantic. Limnol Oceanogr 53: 1722–1733

de la Jara A, Mendoza H, Martel A, Molina C, Nordström L, de la Rosa V, Díaz R (2003) Flow cytometric determination of lipid content in a marine dinoflagellate, *Crypthecodinium cohnii*. J Appl Phycol 15: 433–438

Delia CF, Steudler PA, Corwin N (1977) Determination of total nitrogen in aqueous samples using persulfate digestion. Limnol Oceanogr 22: 760–764

Demers S, Davis K, Cucci TL (1989) A flow cytometric approach to assessing the environmental and physiological status of phytoplankton. Cytometry 10:644–652

Doan TTY, Obbard JP (2011) Enhanced lipid production in *Nannochloropsis* sp. using fluorescence-activated cell sorting. Glob Change Biol Bioenergy 3:264–270

Dodds WK, Strauss EA, Lehmann R (1993) Nutrient dilution and removal bioassays to estimate phytoplankton response to nutrient control. Arch Hydrobiol 128:467–481

Dortch Q, Clayton JR, Thoresen SS, Ahmed SI (1984) Species-differences in accumulation of nitrogen pools in phytoplankton. Mar Biol 81:237–250

Dubelaar GBJ, Jonker RR (2000) Flow cytometry as a tool for the study of phytoplankton. Sci Mar 64:135–156

DuRand MD, Olson RJ (1996) Contributions of phytoplankton light scattering and cell concentration changes to diel variations in beam attenuation in the equatorial Pacific from flow cytometric measurements of pico-, ultra- and nanoplankton. Deep-Sea Res II 43:891–906

DuRand MD, Olson RJ (1998) Diel patterns in optical properties of the chlorophyte *Nannochloris* sp.: relating individual-cell to bulk measurements. Limnol Oceanogr 43:1107–1118

DuRand MD, Green RE, Sosik HM, Olson RJ (2002) Diel variations in optical properties of *Micromonas pusilla* (Prasinophyceae). J Phycol 38:1132–1142

Dusenberry JA, Olson RJ, Chisholm SW (1999) Frequency distributions of phytoplankton single-cell fluorescence and vertical mixing in the surface ocean. Limnol Oceanogr 44:431–436

Eaton A, Clesceri L, Rice E, Greenberg A (2005) Protocol 4500-N C. Persulfate Method. In: APHA, AWWA, WPCF (eds) Standard Methods for the examination of water and wastewater. 21 edn. Amer Public Health Assn

Gouveia L, Marques AE, da Silva TL, Reis A (2009) *Neochloris oleabundans* UTEX #1185: a suitable renewable lipid source for biofuel production. J Ind Microbiol Biotechnol 36:821–826

Graziano LM, Geider RJ, Li WKW, Olaizola M (1996) Nitrogen limitation of North Atlantic phytoplankton: analysis of physiological condition in nutrient enrichment experiments. Aquat Microb Ecol 11: 53–64

Gromping U (2006) Relative importance for linear regression in R: the package relaimpo. J Stat Softw 17(1)

Gromping U (2007) Estimators of relative importance in linear regression based on variance decomposition. Am Stat 61:139–147

Grover JP (1991) Resource competition in a variable environment—phytoplankton growing according to the variable-internal-stores model. Am Nat 138:811–835

Hayes PK, Whitaker TM, Fogg GE (1984) The distribution and nutrient status of phytoplankton in the Southern Ocean between 20° and 70° W. Polar Biol 3:153–165

Hecky R, Kilham P (1988) Nutrient limitation of phytoplankton in freshwater and marine environments: a review of recent evidence on the effects of enrichment. Limnol Oceanogr 33:796–822

Holt RD (2008) Theoretical perspectives on resource pulses. Ecology 89: 671–681

Howarth RW (1988) Nutrient limitation of net primary production in marine ecosystems. Annu Rev Ecol Syst 19:89–110

Hyka P, Lickova S, Pribyl P, Melzoch K, Kovar K (2013) Flow cytometry for the development of biotechnological processes with microalgae. Biotechnol Adv 31:2–16

Ikaran Z, Suárez-Alvarez S, Urreta I, Castañón S (2015) The effect of nitrogen limitation on the physiology and metabolism of *Chlorella vulgaris* var L3. Algal Res 10:134–144

Jacquet S, Lennon JF, Marie D, Vaulot D (1998) Picoplankton population dynamics in coastal waters of the northwestern Mediterranean Sea. Limnol Oceanogr 43:1916–1931

Kass RE, Raftery AE (1995) Bayes factors. J Am Stat Assoc 90:773–795

Kolber Z, Zehr J, Falkowski P (1988) Effects of growth irradiance and nitrogen limitation on photosynthetic energy conversion in Photosystem II. Plant Physiol 88:923–929

Lanoul A, Coleman T, Asher SA (2002) UV resonance raman spectroscopic detection of nitrate and nitrite in wastewater treatment processes. Anal Chem 74:1458–1461

Li G, Brown CM, Jeans JA, Donaher NA, McCarthy A, Campbell DA (2014) The nitrogen costs of photosynthesis in a diatom under current and future pCO. New Phytol 205:533–543

Liu SW, Qiu BS (2012) Different responses of photosynthesis and flow cytometric signals to iron limitation and nitrogen source in coastal and oceanic *Synechococcus strains* (Cyanophyceae). Mar Biol 159: 519–532

Luning K (2005) Endogenous rhythms and daylength effects in macroalgal development. In: Andersen RA (ed) Algal culturing techniques. Elsevier/Academic Press, Burlington, pp 347–364

Malerba ME, Connolly SR, Heimann K (2012) Nitrate-nitrite dynamics and phytoplankton growth: formulation and experimental evaluation of a dynamic model. Limnol Oceanogr 57:1555–1571

Mas S, Roy S, Blouin F, Mostajir B, Therriault JC, Nozais C, Demers S (2008) Diel variations in optical properties of *Imantonia rotunda* (Haptophyceae) and *Thalassiosira pseudonana* (Bacillariophyceae) exposed to different irradiance levels. J Phycol 44:551–563

Mulholland MR, Lomas MW (2008) Nitrogen uptake and assimilation. In: Capone DG, Bronk DA, Mulholland MR, Carpenter EJ (eds) Nitrogen in Marine Environment, 2nd edn. Elsevier, Amsterdam, pp 303–384

Nichols HW (1973) Growth media - freshwater. In: Stein J (ed) Handbook of phycological methods. Cambridge University Press, Cambridge, pp 7–24

Olson RJ, Shalapyonok A, Sosik HM (2003) An automated submersible flow cytometer for analyzing pico- and nanophytoplankton: FlowCytobot. Deep-Sea Res I 50:301–315

Raimbault P, Diaz F, Pouvesle W, Boudjellal B (1999) Simultaneous determination of particulate organic carbon, nitrogen and phosphorus collected on filters, using a semi-automatic wet-oxidation method. Mar Ecol Prog Ser 180:289–295

Rodolfi L, Zittelli GC, Bassi N, Padovani G, Biondi N, Bonini G, Tredici MR (2009) Microalgae for oil: strain selection, induction of lipid

synthesis and outdoor mass cultivation in a low-cost photobioreactor. Biotechnol Bioeng 102:100–112

Roenneberg T, Mittag M (1996) The circadian program of algae. Semin Cell Dev Biol 7:753–763

RStudio (2013) version 0.98.507, Boston (MA), url http://www.rstudio.org/

Schwarz GE (1978) Estimating the dimension of a model. Ann Stat 6: 461–464

Shelly K, Holland D, Beardall J (2010) Assessing nutrient status of microalgae using chlorophyll *a* fluorescence. In: Suggett DJ, Borowitzka M, Prášil O (eds) Chlorophyll *a* fluorescence in aquatic sciences methods and applications. Springer, Dordrecht, pp 223–236

Solorzano L, Sharp JH (1980) Determination of total dissolved nitrogen in natural-waters. Limnol Oceanogr 25:751–754

Sosik HM, Chisholm SW, Olson RJ (1989) Chlorophyll fluorescence from single cells—interpretation of flow cytometric signals. Limnol Oceanogr 34:1749–1761

Sosik HM, Olson RJ, Armbrust EV (2010) Flow cytometry in phytoplankton research. In: Suggett DJ, Borowitzka M, Prášil O (eds) Chlorophyll *a* fluorescence in aquatic sciences methods and applications. Springer, Dordrecht, pp 171–186

Strong DR, Whipple AV, Child AL, Dennis B (1999) Model selection for a subterranean trophic cascade: root-feeding caterpillars and entomopathogenic nematodes. Ecology 80:2750–2761

Thyssen M, Gregori GJ, Grisoni JM, Pedrotti ML, Mousseau L, Artigas LF, Marro S, Garcia N, Passafiume O, Denis MJ (2014) Onset of the spring bloom in the northwestern Mediterranean Sea: influence of environmental pulse events on the in situ hourly-scale dynamics of the phytoplankton community structure. Front Microbiol 5:387. doi: 10.3389/fmicb.2014.00387

Timmermans KR, Davey MS, Bvd W, Snoek J, Geider RJ, Veldhuis MJW, Gerringa LJA, Baar HJW (2001) Co-limitation by iron and light of *Chaetoceros brevis*, *C. dichaeta* and *C. calcitrans* (Bacillariophyceae). Mar Ecol Prog Ser 217:287–297

Turpin DH (1991) Effects of inorganic N availability on algal photosynthesis and carbon metabolism. J Phycol 27:14–20

Vanucci S, Guerrini F, Milandri A, Pistocchi R (2010) Effects of different levels of N- and P-deficiency on cell yield, okadaic acid, DTX-1, protein and carbohydrate dynamics in the benthic dinoflagellate *Prorocentrum lima*. Harmful Algae 9:590–599

Veldhuis MJW, Kraay GW (2000) Application of flow cytometry in marine phytoplankton research: current applications and future perspectives. Sci Mar 64:121–134

von Dassow P, van den Engh G, Iglesias-Rodriguez D, Gittins JR (2012) Calcification state of coccolithophores can be assessed by light scatter depolarization measurements with flow cytometry. J Plankton Res 34:1011–1027

Yentsch CM, Horan PK, Muirhead K, Dortch Q, Haugen E, Legendre L, Murphy LS, Perry MJ, Phinney DA, Pomponi SA, Spinrad RW, Wood M, Yentsch CS, Zahuranec BJ (1983) Flow-cytometry and cell sorting—a technique for analysis and sorting of aquatic particles. Limnol Oceanogr 28:1275–1280

Zettler ER, Olson RJ, Binder BJ, Chisholm SW, Fitzwater SE, Gordon RM (1996) Iron-enrichment bottle experiments in the equatorial Pacific: responses of individual phytoplankton cells. Deep Sea Res II 43:1017–1029

Zhou Q, Chen W, Zhang H, Peng L, Liu L, Han Z, Wan N, Li L, Song L (2012) A flow cytometer based protocol for quantitative analysis of bloom-forming cyanobacteria (*Microcystis*) in lake sediments. J Environ Sci (China) 24(9):1709–1716

Zuur A, Ieno EN, Walker N, Saveliev AA, Smith GM (2009) Mixed effects models and extensions in ecology with R. Springer, New York